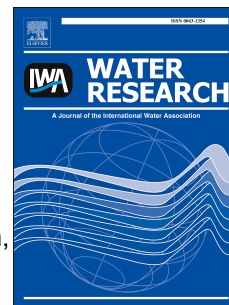


# Journal Pre-proof

Process design tools and techno-economic analysis for capacitive deionization

Tristan D. Hasseler, Ashwin Ramachandran, William A. Tarpeh, Michael Stadermann,  
Juan G. Santiago



PII: S0043-1354(20)30571-6

DOI: <https://doi.org/10.1016/j.watres.2020.116034>

Reference: WR 116034

To appear in: *Water Research*

Received Date: 28 March 2020

Revised Date: 4 June 2020

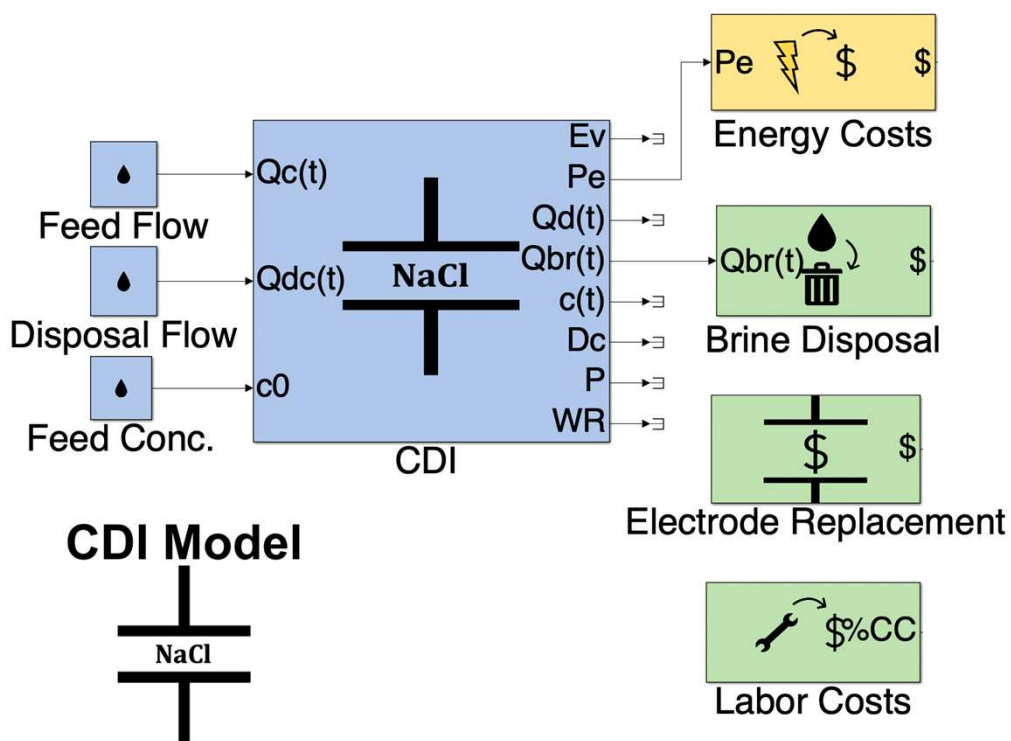
Accepted Date: 8 June 2020

Please cite this article as: Hasseler, T.D., Ramachandran, A., Tarpeh, W.A., Stadermann, M., Santiago, J.G., Process design tools and techno-economic analysis for capacitive deionization, *Water Research* (2020), doi: <https://doi.org/10.1016/j.watres.2020.116034>.

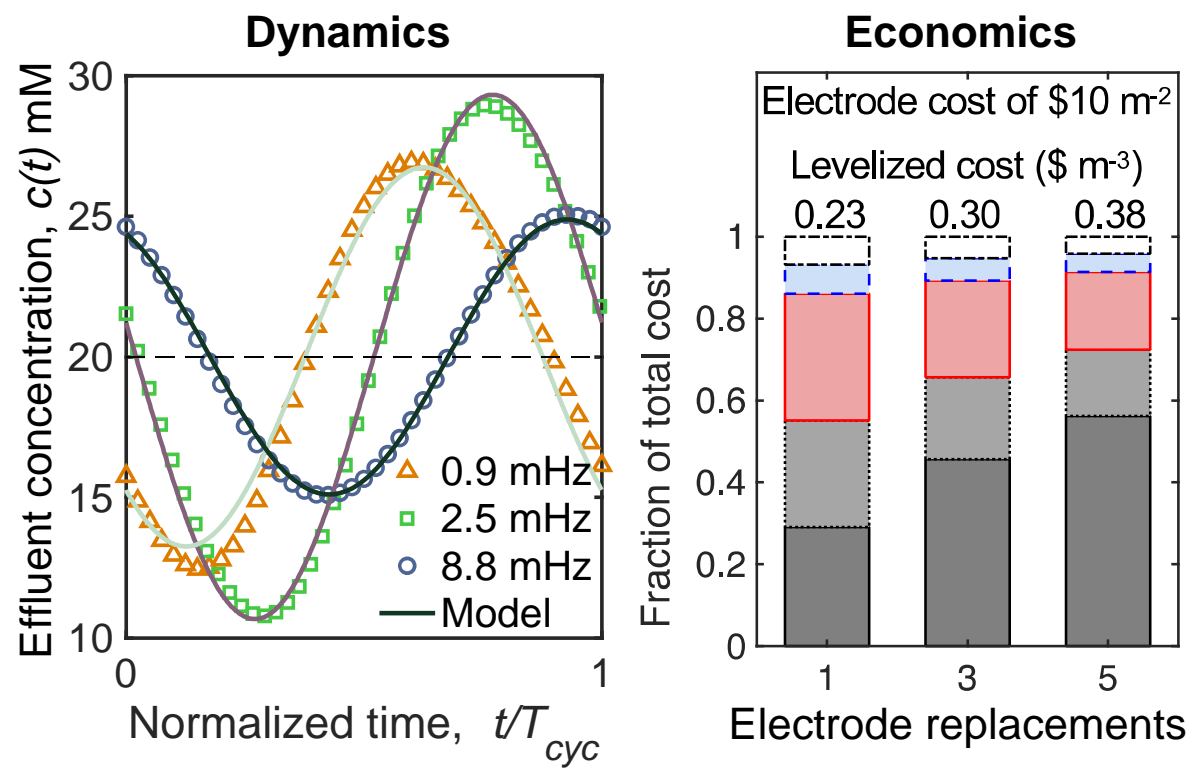
This is a PDF file of an article that has undergone enhancements after acceptance, such as the addition of a cover page and metadata, and formatting for readability, but it is not yet the definitive version of record. This version will undergo additional copyediting, typesetting and review before it is published in its final form, but we are providing this version to give early visibility of the article. Please note that, during the production process, errors may be discovered which could affect the content, and all legal disclaimers that apply to the journal pertain.

© 2020 Published by Elsevier Ltd.

## 1. Model specification



## 2. Model simulation



## Process design tools and techno-economic analysis for capacitive deionization

Tristan D. Hasseler,<sup>a</sup> Ashwin Ramachandran,<sup>a</sup> William A. Tarpeh,<sup>b</sup> Michael Stadermann,<sup>c</sup> Juan G. Santiago<sup>d,\*</sup>

<sup>a</sup> Department of Aeronautics & Astronautics, Stanford University, Stanford, California 94305, United States

<sup>b</sup> Department of Chemical Engineering, Stanford University, Stanford, California 94305, United States

<sup>c</sup> Lawrence Livermore National Laboratory, 7000 East Avenue, Livermore, CA, 94550, United States

<sup>d</sup> Department of Mechanical Engineering, Stanford University, Stanford, California 94305, United States

\* To whom correspondence should be addressed. Tel. 650-736-1283, Fax 650-723-7657, E-mail: [juan.santiago@stanford.edu](mailto:juan.santiago@stanford.edu)

### Abstract

Capacitive deionization (CDI) devices use cyclical electrosorption on porous electrode surfaces to achieve water desalination. Process modeling and design of CDI systems requires accurate treatment of the coupling among input electrical forcing, input flow rates, and system responses including salt removal dynamics, water recovery, energy storage, and dissipation. Techno-economic analyses of CDI further require a method to calculate and compare between a produced commodity (e.g. desalted water) versus capital and operational costs of the system. We here demonstrate a new modeling and analysis tool for CDI developed as an installable Matlab program that allows direct numerical simulation of CDI dynamics and calculation of key performance and cost parameters. The program is provided for free and is used to run open-source Simulink models. The Simulink environment sends information to the program and allows for a drag and drop design space where users can connect CDI cells to relevant periphery blocks such as grid energy, battery, solar panel, waste disposal, and maintenance/labor cost

streams. The program allows for simulation of arbitrary current forcing and arbitrary flow rate forcing of one or more CDI cells. We employ validated well-mixed reactor formulations together with a non-linear circuit model formulation that can accommodate a variety of electric double layer sub-models (e.g. for charge efficiency). The program includes a graphical user interface (GUI) to specify CDI plant parameters, specify operating conditions, run individual tests or parameter batch-mode simulations, and plot relevant results. The techno-economic models convert among dimensional streams of species (e.g. feed, desalted water, and brine), energy, and cost and enable a variety of economic estimates including levelized water costs.

Keywords: water desalination; capacitive deionization; process design tool; variable flow; electrode aging; techno-economic analysis

## 1. Introduction

Capacitive deionization (CDI) is a rapidly developing water desalination technology that uses multiple porous electrode pairs in a configuration similar to a supercapacitor to electrostatically trap salt ions (Oren, 2008; Suss et al., 2015). CDI has been identified as a potential replacement for traditional large-scale water desalination processes such as reverse osmosis (RO) for feedwater with salinity significantly lower than sea water, such as brackish water with salt concentrations less than roughly  $10 \text{ g L}^{-1}$ . (Oren, 2008; Suss et al., 2015). CDI has also been demonstrated and applied to the selective removal of ionic impurities including nitrate (Oyarzun et al., 2018). To establish CDI as a viable technology for brackish water desalination, research has mostly focused on developing and assessing operational modes for CDI (Kim and Yoon, 2015). A subset of this work has sought to optimize the design and/or operation of CDI cells

under specified performance constraints (Demirer et al., 2013; Wang and Lin, 2019). Recently, a set of standard performance metrics (namely, water recovery  $WR$ , volume-averaged average desalination depth  $\Delta c$  [mM], productivity  $P$  [ $\text{L h}^{-1} \text{m}^{-2}$ ] and volumetric energy consumption  $E_v$  [ $\text{kWh m}^{-3}$ ]) have been developed (Hawks et al., 2019) to enable direct quantitative evaluation of CDI operating schemes and comparison with other water technologies. For constant feed flow rates, this treatment has been applied to constant voltage (CV) and constant current (CC) operation to assess key contributors to operating costs, for example energy consumption (Hemmatifar et al., 2016; Qu et al., 2016; Dykstra et al., 2018; Qin et al., 2019; Ramachandran et al., 2019; Hand et al., 2019b). Recently, similar treatments have also been extended to sinusoidal voltage and current electrical inputs (Ramachandran et al., 2018a).

The aforementioned simple comparisons of energy-related operating costs are insufficient to compare among the many desalination technologies. In addition to other operating costs (such as brine disposal, labor, and electrode replacements), there are other initial capital investment costs such as CDI plant components, power electronics, and any capacitive energy recovery components (e.g. see Oyarzun et al., 2020). Notably, Hand et al. (2019a) presented a techno-economic study of CDI which included a detailed framework for sizing and pricing CDI and membrane CDI cells. Hand et al. explored a fairly wide CDI design space for constant flow rate given CC operation and found the additional material and capital costs greatly outweigh operational costs. This initial study by Hand et al. encourages further and more comprehensive analysis of capital cost mitigation—particularly exploration of the complex coupling between operational modes, electrode costs, and electrode aging. Also useful would be an easy-to-use and open source modeling tool to enable simulations of one or more CDI cells and their interaction

with ancillary systems (e.g. power conversion units or brine disposal method) to determine balances among streams of cost, energy, and species.

We present an experimentally validated CDI dynamics and techno-economic simulation program for development and assessment of novel CDI systems. We developed an open-source Matlab program with an intuitive graphical user interface (GUI) which allows simulation of effluent concentration dynamics coupled with electric double layer (EDL) and Faradaic efficiencies, calculation of cycle performance parameters, and full economic analyses. In contrast to the previous work mentioned, where flow rates and electrical input were held constant, our program allows fairly arbitrary temporal variations of electrical and flow rate forcing functions. We demonstrate the program to study effluent concentration dynamics in response to sinusoidal flow rate and current inputs. We vary the amplitude and phase of the sinusoidal flow rate to explore a wide parameter design space for sinusoidal flow rate inputs and calculate resulting cell performance parameters within the space. The program's ability to deal with arbitrary electrical input and flow rate input enables exploration of complex trade-offs among important figures of merit.

We further use our program to perform an example techno-economic analysis of CDI, considering the relative effects of capital costs, operating costs, and electrode aging mechanisms on the net levelized cost of water. To this end, we consider three separate electrode aging hypotheses (two in the main paper and one in the Supplementary Information, SI, document). These hypotheses are encoded into the program as possible electrode replacement criteria (see Lu et al., 2017; Liu et al., 2019). In this way, we study the relative effect of electrode lifetime on the overall produced water cost for a number of different electrode unit costs. For present-day

constituent material cost estimates, we find that capital and material costs are more dominant than operating costs over the lifetime of a non-membrane CDI plant.

## 2. Theory

### 2.1. Well-mixed reactor model with extendable electric double layer formulations

For salt removal dynamics, we model the CDI cell as a well-mixed reactor coupled with a non-linear RC circuit formulation based on the experimentally validated model of Ramachandran et al. (2018a). Applying a salt mass balance over the cell volume yields the well-mixed reactor formulation for salt concentration dynamics

$$\tau(t) \frac{d(\Delta c(t))}{dt} + \Delta c(t) = \frac{I(t) \lambda_c \lambda_{dl}}{FQ(t)}. \quad (1)$$

Here  $I(t)$  is the current supplied to the cell,  $Q(t)$  is the flow rate of fluid through the cell, and  $\Delta c(t) \equiv c_0 - c(t)$  is the instantaneous salt concentration reduction from the feed concentration,  $c_0$ .  $\tau(t) \equiv V/Q(t)$  is a time scale proportional to the flow residence time as a function of the mixed reactor cell volume  $V$  and the instantaneous flow rate  $Q(t)$ .  $F$  is Faraday's constant, and  $\lambda_c$  and  $\lambda_{dl}$  are respectively the Coulombic and differential charge efficiencies (Ramachandran et al., 2018a, 2018b). The values of  $\lambda_{dl}$  reflect the treatment of electric double layer physics at the electrodes. Two commonly used formulations are the modified Donnan (mD) (Biesheuvel et al., 2011) and Guoy-Chapman-Stern (GCS) (Biesheuvel et al., 2009) models. For simplicity, we here treat  $\lambda_{dl}$  as a simple numerical input reflecting the appropriate cycle-averaged value, represented as  $\overline{\lambda_{dl}}$  (see discussion and calculations by Ramachandran et al., 2018b). We note that the current modeling program can be reconfigured to accommodate virtually any model for  $\overline{\lambda_{dl}}$ . We present

a detailed discussion on selecting a cycle-averaged value for  $\overline{\lambda_{dl}}$  for a given operational voltage window in Section S2 of the SI document.

Similarly, our model uses a single, cycle-averaged value of Coulombic efficiency  $\lambda_c$ . The latter treatment is motivated by the work of Hawks et al. (2018) and Ramachandran et al. (2018b) who showed that  $\lambda_c$ , which is governed by leakage currents (Faradaic charge-transfer reactions) at high voltage potentials, can be estimated using preliminary experimental data for the cell. See for example Fig. S5 and associate discussion in the SI of Hawks et al. (2019).

## 2.2. Performance metrics to assess the operation of CDI cells

Presented here is a formulation of four key parameters critical in analyzing the engineering performance of a CDI design and its mode of operation. These figures of merit were described in detail in a multi-laboratory review of CDI performance quantification (Hawks et al., 2019).

First, the water recovery ratio,  $WR$ , is a non-dimensional measure of the quantity of desalinated water produced for a given total volume of water processed. It can be calculated as

$$WR \equiv \frac{\mathcal{V}_{desal}}{\mathcal{V}_{desal} + \mathcal{V}_{waste}}. \quad (2)$$

The volume of desalinated water and waste brine water produced per cycle are respectively calculated as

$$\mathcal{V}_{desal} = \int_{T_{cyc}, \Delta C > 0} Q_{desal}(t) dt,$$

$$\mathcal{V}_{waste} = \int_{T_{cyc}, \Delta C < 0} Q_{waste}(t) dt.$$



$Q_{desal}(t)$  and  $Q_{waste}(t)$  are arbitrary time-varying functions describing the flow rate passed through the cell during desalination ( $\Delta c > 0$ ) and electrode regeneration ( $\Delta c < 0$ ), respectively. The limits of these integrals indicate that we consider a specific instantaneous output salt concentration as delimiting the start and end of the adsorption and desorption phases of the cycle. Note the choice of this salt concentration limit determines the value of  $WR$ .

Second, the productivity,  $P$  [ $\text{L h}^{-1} \text{m}^{-2}$ ], of the CDI stack quantifies throughput and is defined as the volume of desalinated water,  $\mathcal{V}_{desal}$ , produced per time and per total electrode area as follows:

$$P \equiv \frac{\mathcal{V}_{desal}}{N_e A_e T_{cyc}}. \quad (3)$$

Here,  $N_e$  is the number of single electrodes in the CDI stack,  $A_e$  is the projected facial surface area of a single electrode, and  $T_{cyc}$  is the cycle time (i.e. including adsorption and desorption phases).

Third, the volume-averaged concentration reduction,  $\Delta c$  (expressed in mM), is a measure of the volume-averaged desalination depth as

$$\Delta c \equiv \frac{N_{desal}}{\mathcal{V}_{desal}}. \quad (4)$$

Note in this work we differentiate volume-averaged desalination depth  $\Delta c$  from instantaneous desalination depth  $\Delta c(t)$  through omission of  $(t)$ .  $N_{desal}$  is the number of moles of salt removed in the adsorption phase where

$$N_{desal} = \int_{T_{cyc}, \Delta c > 0} Q_{desal}(t) \cdot \Delta c(t) dt.$$

Lastly, the volumetric energy consumption,  $E_v$  [kWh m<sup>-3</sup>], represents the energy used to produce a given volume of desalinated water as follows:

$$E_v \equiv \frac{E_{charge} - \eta E_{discharge}}{V_{desal}}. \quad (5)$$

For simplicity, we treat  $\eta \in [0,1]$  as a user-specified energy recovery efficiency factor which governs how much energy can be recovered by the system during the discharging phase (see Oyarzun et al., 2020 for a detailed discussion of energy recovery efficiency in CDI). The energy consumed (recovered) during charging (discharging) are respectively

$$E_{charge} = \int_{T_{cyc}, I > 0} I(t) \cdot V_{cell}(t) dt,$$

$$E_{discharge} = \int_{T_{cyc}, I < 0} I(t) \cdot V_{cell}(t) dt.$$

Here  $V_{cell}(t)$  is the instantaneous voltage potential across the cell. Note that other formulations of other performance paramers, such as average salt adsorption rate (ASAR), can be derived from the performance parameters above (see Hawks et al., 2019).

### 2.3. Techno-economic analysis of CDI systems

The techno-economic analysis of CDI includes conversions among streams of species, energy, and costs and includes comparisons among future, recurring, and present costs. As per standard present-worth of cost analysis (Newman et al., 2015), each future expense  $F_c$  incurred  $n$  interest periods in the future is converted to an equivalent present cost  $P_c$  through

$$P_c = \frac{F_c}{(1+i)^n}. \quad (6)$$

Here  $i$  is the discount rate assumed for the analysis. This rate can be used to account for interest, inflation, and other factors and can be compared to the rate of return of competing investments

(Newman et al., 2015). Similarly, a set of regularly occurring uniform payments  $A$  incurred for  $n$  periods is converted to a single present-day cost using

$$P_c = A \frac{(1+i)^n - 1}{i(1+i)^n}. \quad (7)$$

Note the pre-factor obtained from inverting this equation is defined as the fixed charge rate,  $FCR \equiv [\frac{(1+i)^n - 1}{i(1+i)^n}]^{-1}$ . In our analysis, the FCR is determined from the user-selected value for  $i$  and is a parameter used to compute the total levelized cost of produced (desalted) water,  $LC$  as follows:

$$LC [\text{\$ m}^{-3}] = \frac{\sum_{i=1}^N [(CC_i \cdot FCR) + A_i]}{\mathcal{V}_{tot}} \quad (8)$$

where  $CC$  is a capital cost and  $\mathcal{V}_{tot}$  is the total volume of desalinated water produced over a specified timeframe. This relation describes the summation of all distributed costs over a given time period (typically annually) and normalizing by the volume of desalted water produced over that period. See for example Bartholomew et al. (2018) and Hand et al. (2019a) for similar techno-economic analyses applied respectively to osmotically assisted reverse osmosis (OARO) and CDI (both with and without membranes).

### 3. Open-source Matlab graphical user interface (GUI) program for CDI process design and techno-economic analysis

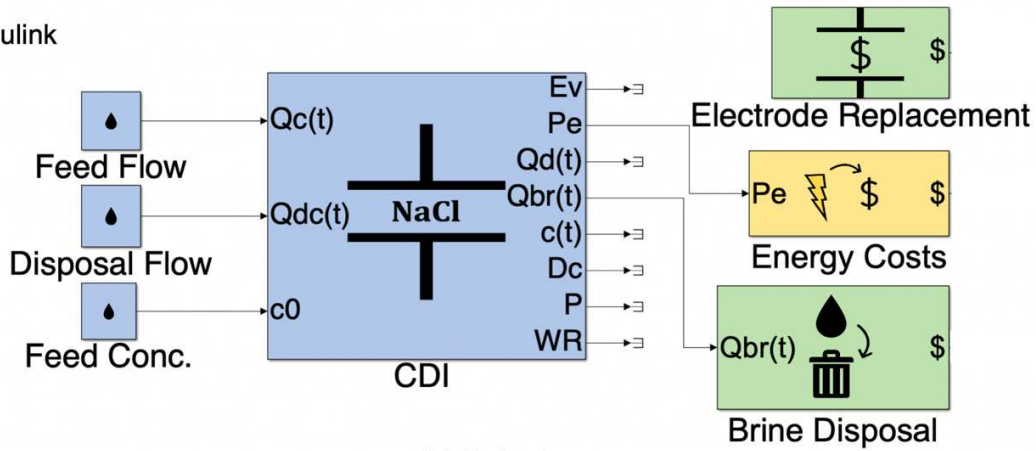
#### 3.1. CDI system specification through drag and drop design in Simulink

To specify CDI plant configurations, the user chooses from among a set of pre-constructed Simulink blocks provided in the open source “CDI\_Block\_Library.slx” file. Icons are arranged in Simulink via drag and drop to connect CDI cells to desired peripheries including power and water feed systems. Once a CDI configuration is specified in Simulink, our GUI Matlab program

is used to run the model and view results. The fully modular nature of the Simulink environment allows simulation of CDI cells in context with other auxiliary non-water systems. For example, a CDI system can be developed which draws electricity from solar panels and disposes of wastewater into a sink (i.e. disposal method) which has varying costs based on waste concentration. Once blocks are connected, lines represent flows of species, energy, and cost, and the program automatically converts dimensions between flows. Further, the program mimics CDI operation in real-world time, meaning the plant is simulated to run each day of the year for a specified operational schedule. In this way, peripheries such as electricity costs can be modeled as the real-time energy costs (which vary throughout the day and the seasons) specific to a given location (in our study, we use published electricity prices for the San Francisco, CA Bay Area, PG&E, 2019). A user manual for the CDI program which outlines best practices for using Simulink and the GUI can be found in Section S3 of the SI. Fig. 1a shows how a configuration that includes waste disposal, energy requirements, and electrode replacement can be designed in

214 Simulink.

(a) Simulink



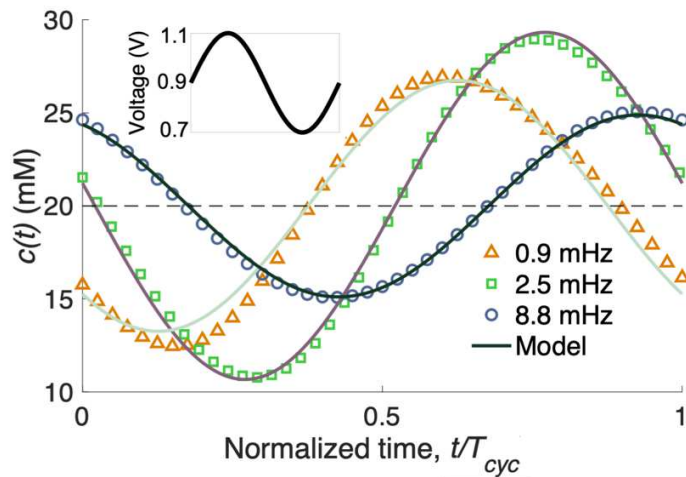
(b) GUI

**User Inputs**

CDI Plant	
Capacitance to cell vol.	44 F cm <sup>-3</sup>
Resistance to elec. area	57 Ohm cm <sup>2</sup>
Cell volume by area	0.00107 m <sup>3</sup> m <sup>-2</sup>
# of electrode pairs	5
Surface area, electrode	19.635 cm <sup>2</sup>
Electrode thickness	0.03 cm
Internal area by mass	500 m <sup>2</sup> g <sup>-1</sup>
Mass per electrode	0.2 g
Power recovery eff.	0 %

**Run Model**

(c) Outputs



215

216 **Fig. 1.** Overview of CDI physics and techno-economic program including drag-and-drop icons in  
 217 Simulink (a), an example GUI input table (b), and experimentally validated model output (c).  
 218 The MathWorks Simulink environment is used to configure a CDI plant. Icons represent transfer  
 219 functions in a dynamic (unsteady) simulation. Example system shown operates on grid power  
 220 and includes a wastewater disposal cost transfer function. (b) GUI includes input tables to  
 221 specify plant parameters and input control schemes. Values shown here are consistent with the  
 222 experimental data of Ramachandran et al. (2018a). (c) Example output predictions of CDI model.  
 223 Plotted as solid curves are predicted effluent salt concentration (solid curves) compared to

experimental data (symbols) of Ramachandran et al. (2018a) for constant flow rate, sinusoidal voltage forcing functions (inset) at frequencies of 0.9 (red triangles), 2.5 (green squares), and 8.8 mHz (blue circles).

### *3.2. CDI cell parameters, operational parameter inputs, and graphical outputs in the GUI*

Once a user has specified a CDI configuration in Simulink, the GUI Matlab program (e.g. Fig. 1b) can be used to specify physical CDI plant parameters such as cell resistance, capacitance, and volume; operating conditions (e.g. current forcing functions, flow rate functions, number of cycles); and economic input parameters (e.g. discount rates, operation schedules, capital costs). Once the simulation has been executed, the GUI program is also used to display results of the techno-economic analysis, including cycle performance parameters, volume of clean water produced, time-varying concentration responses, and full economic cost breakdowns in addition to the levelized cost of desalinated water.

Users can run standalone dynamics simulations (with or without economic analysis) as well as full parameter sweep batch simulations. In parameter batch simulations, any number of variables are specified as vectors over which they are varied. The CDI program sequentially runs a simulation for each variable permutation, and all relevant results are stored in a data structure for later use. See Section S3.6 in the SI for further discussion on specifying and running parameter batch simulations. In this regard, the program allows preliminary sensitivity and trade-off studies for any parameter of choice. We use this functionality in Section 4.1 to study the performance of sinusoidal flow rate operation within a parameter design space.

### *3.3. Validation of current model predictions with experimental data from lab-scale experiments*

Curves of model-predicted effluent concentrations are shown in Fig. 1c as solid curves. These predictions compare very well with experimental data of Ramachandran et al. (2018a). Shown are cases of sinusoidal voltage forcing at frequencies of 0.9, 2.5, and 8.8 mHz and constant feed flow rate. Cell parameters reported by Ramachandran et al. (2018a) were used to specify the physical CDI inputs and are consistent with those shown in Fig. 1b. See Section S1 in the SI for a complete list of cell parameters and detailed discussion of operational conditions and assumptions.

Users are warned by the program if an operating scheme causes certain model assumptions to be violated. These include conditions for the well-mixed reactor, realistic constant resistance and capacitance values, and assumptions regarding cycle efficiencies. See Sections S1 and S3.3 in the SI for more information on running the program within the model's limits.

#### 4. Results & Discussion

We here present example applications of our validated CDI program to a study of CDI effluent salt concentration in response to complex forcing functions and a techno-economic analysis of electrode cost relative to total levelized water costs. Table 1 presents a complete list of the CDI plant parameters used for these and all subsequent modeling studies presented in this paper unless otherwise specified. The values are consistent with the system discussed in detail by Ramachandran et al (2018a).

**Table 1.** CDI plant parameters used in simulations

Parameter	Value
Effective resistance, $R$	2.9 $\Omega$

Resistance normalized by electrode surface area, $\bar{R}$	$57 \Omega \cdot \text{cm}^2$
Effective capacitance, $C$	$32.4 \text{ F}$
Capacitance normalized by electrode volume, $\bar{C}$	$44 \text{ F cm}^{-3}$
Cell volume, $\forall$	$2.1 \text{ mL}$
Projected surface area of a single electrode, $A_e$	$19.64 \text{ cm}^2$
Number of electrode pairs	$5$
Internal porous area of a single electrode, $a$	$500 \text{ m}^2 \text{ g}^{-1}$
Mass of a single electrode	$0.2 \text{ g}$
Electrode thickness, $\delta$	$0.03 \text{ cm}$
Power recovery efficiency, $\eta$	$0\%$
Effective dynamic charge efficiency, $\bar{\Lambda} \equiv \bar{\lambda}_{dl} \lambda_c$	$0.80$

269

270 *4.1. Simulations of variable flow rate and variable applied current operations*

271 We here consider a cell subject to sinusoidal input current. We further consider a flow rate  
272 forcing function composed of a constant value plus a sinusoidal component with both varying  
273 amplitude and phase. The sinusoidal current forcing is described by  $I(t) = \Delta I \cdot \sin(\omega t)$  where  
274  $\Delta I = 70 \text{ A m}^{-2}$  and the sinusoidal flow rate is described by  $Q(t) = Q_{dc} + \Delta Q \cdot \sin(\omega t + \phi)$   
275 where  $Q_{dc} = 4 \text{ L m}^{-2} \text{ min}^{-1}$ . Fig. 2a and 2b respectively show plots of effluent concentration  
276 versus normalized time ( $t/T_{cyc}$ ) for several values of magnitude ( $\Delta Q/Q_{dc} = 0, 0.5, 1$ ) and phase  
277 ( $\phi = 0, \frac{\pi}{2}, \pi$  rads). Drawing from Ramachandran et al. (2018a), we chose a current and flow rate  
278 frequency  $\omega = 0.026 \text{ rad/s}$  that corresponds to resonance for the constant (DC) flow rate  
279 component,  $\omega_{res} = 1/\sqrt{\tau RC}$ , where here  $\tau \equiv \forall/Q_{dc} = 16.1 \text{ s}$ . We note that there is no known  
280 CDI resonance criterion for the present case of time-varying flow rate.



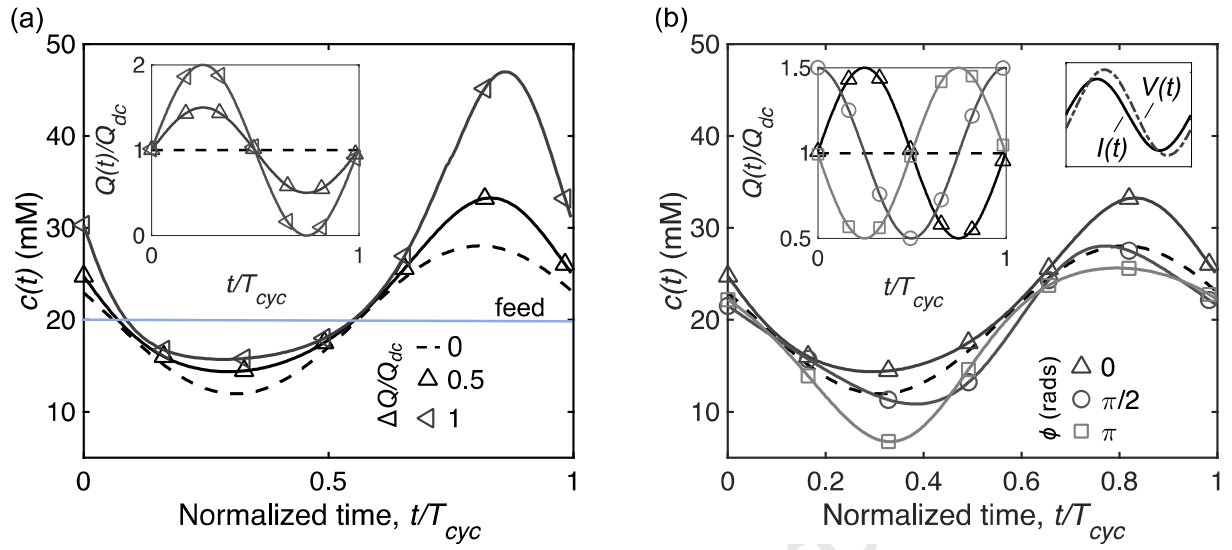


**Fig. 2.** Effects of varying amplitude of sinusoidal flow rate component  $\Delta Q$  (a) and phase  $\phi$  (b) on CDI effluent concentration versus time,  $c(t)$ . All curves are responses to the same sinusoidal current forcing function with a maximum resulting peak-to-peak cell voltage of 0.8 V and a feed concentration fixed at 20 mM. Flow rate is  $Q(t) = Q_{dc} + \Delta Q \cdot \sin(\omega t + \phi)$  where  $Q_{dc} = 4 \text{ L m}^{-2} \text{ min}^{-1}$ .  $\omega = 0.026 \text{ rad/s}$  is the CDI resonant frequency for the case of  $Q = Q_{dc}$ . (a) shows flow rate amplitudes  $\Delta Q/Q_{dc}$  of 0, 0.5, and 1 for zero phase offset. (b) shows phase offsets of 0,  $\pi/2$ , and  $\pi$  radians for  $\Delta Q/Q_{dc} = 0.5$ . In both (a) and (b), the dashed black curve is the response for a baseline constant flow rate of  $4 \text{ L m}^{-2} \text{ min}^{-1}$  ( $\Delta Q = 0$ ). Marker shapes correspond to specific values of  $\Delta Q/Q_{dc}$  and  $\phi$  within the more comprehensive contour plots of Fig. 3.

Fig. 2a isolates the effect of flow rate amplitude on desalination depth. Higher flow rate amplitude in phase with the desalination period implies less desalination (sacrificing salt removal for increased instantaneous productivity). Conversely, lower flow rate amplitude in phase with regeneration results in higher brine concentration. The latter sacrifices instantaneous productivity for improved water recovery ratio. The combined effects of in-phase flow rate amplitude are

therefore higher water recovery ratio, high productivity, and lower energy consumption (per volume of produced water) at the expense of a low cycle-averaged desalination depth. Fig. 2b isolates the effect of phase change for a single case of flow rate amplitude ( $\Delta Q/Q_{dc} = 0.5$ ). We observe that instantaneous concentration deviation from the inlet value increases as current-to-flow-rate phase difference increases from 0 to  $\pi$  radians. Thus, a low (high) flow rate in phase with desalination (regeneration) decreases (increases) instantaneous output concentration. This has a significant effect on all of the figures of merit discussed in Section 2.2. Overall, increasingly out-of-phase flow rate results in improved  $\Delta c$  but the relatively low flow rates during desalination result in decreased  $WR$ ,  $P$ , and  $E_v$ .

Fig. 3 presents a more comprehensive analysis of the effects of flow rate sinusoid amplitude and phase on the aforementioned figures of merit for CDI. The axes of the contours of Fig. 3 span all values of  $\frac{\Delta Q}{Q_{dc}} \in [0,1]$  and  $\phi \in [0,\pi]$  radians. Plots (a) through (d) show quantitative predictions of performance measures  $WR$ ,  $\Delta c$ ,  $P$ , and  $E_v$  respectively. Note that  $\phi$  is limited to  $\pi$  radians, as the performance parameters are identically mirrored about the  $\phi = \pi$  axis. Regions marked as “not feasible” represent operating conditions where effluent concentration approaches 0 mM during desalination (complete desalination) or applied voltage exceeds 1.2 V (Faradaic limits of water splitting), violating the assumptions of the model.

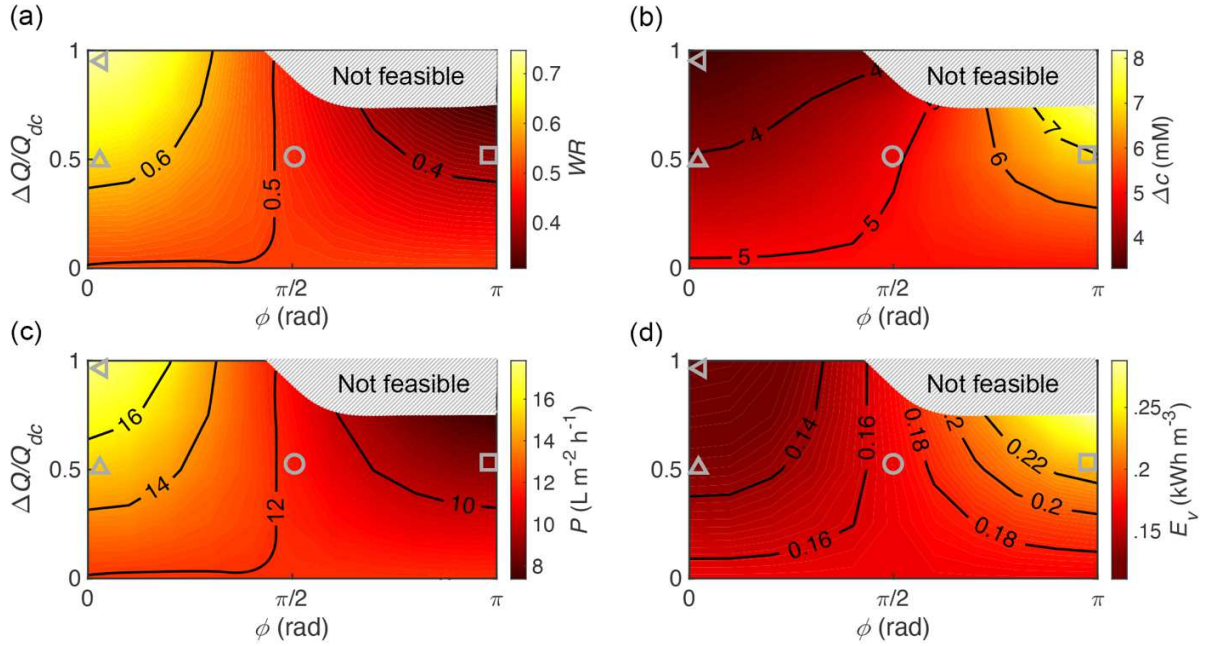


**Fig. 3.** Key performance metrics for sinusoidal current and a flow rate of the form  $Q(t) = Q_{dc} + \Delta Q \cdot \sin(\omega t + \phi)$  as a function of  $\phi$  and  $\Delta Q$  for  $Q_{dc} = 4 \text{ L m}^{-2} \text{ min}^{-1}$ . The current is described by  $I(t) = \Delta I \cdot \sin(\omega t)$ , with  $\Delta I = 70 \text{ A m}^{-2}$ ,  $\omega = 0.026 \text{ rad/s}$ , and  $0.8 \text{ V}$  as the maximum resulting peak-to-peak cell potential and  $c_0 = 20 \text{ mM}$ . Contours show values of water recovery  $WR$  (a), volume-averaged desalination depth  $\Delta c$  (b), productivity  $P$  (c), and volumetric energy consumption  $E_v$  (d). Grey symbols correspond to the cases of Fig. 2. The horizontal triangles mark regions of most favorable  $WR$ ,  $P$ , and  $E_v$  (maximum  $WR$  and  $P$ ; minimum  $E_v$ ) and least favorable  $\Delta c$  (minimum  $\Delta c$ ). Hence,  $\Delta c$  is optimized at the expense of the other measures.

Fig. 3 shows clearly the tradeoff between water recovery, productivity, and energy consumption on one hand and desalination depth on the other. As before, low instantaneous flow rate in phase with the regeneration period favors higher concentration duration desalination and higher brine concentration, collectively favoring  $WR$ ,  $P$ , and  $E_v$ . In contrast, the highest desalination depth is achieved with a sinusoidal flow rate that is a half period out of phase with current. This

minimizes the volume of produced (desalted) water. Note the tradeoff between desalination depth and the other parameters also holds for a constant value of flow rate. We note that these results and insights are limited to the case of both sinusoidal flow rate and current. We hypothesize that a much more generalized study of these tradeoffs would require considerations of arbitrary shape as well as phase. We suggest that such optimizations may significantly benefit from the simulation program presented here.

#### *4.2. Techno-economic analysis: Assessing fractional impact of electrode replacement cost to overall levelized water cost*

We here present an example techno-economic analysis considering the contribution of electrode cost to the net levelized cost of water produced by CDI. We will also consider several criteria for electrode aging and replacement. CDI electrode costs are a significant fraction of total cost in CDI and so we will consider them a special category of cost apart from more typical capital or operational costs.

We first consider electrode costs ranging from  $\$1 \text{ m}^{-2}$  to  $\$10 \text{ m}^{-2}$ . The  $\$10 \text{ m}^{-2}$  value is closest to what is currently attainable for complete electrodes (carbon, binder, conductivity additive) in industry (Hand et al., 2019a), while the lower values represent future possible values given advancements in fabrication and increase of the scale of production. We will term capital costs as non-electrode but CDI-specific construction of plant costs (frames/housing, current collectors, etc.). We conservatively increase capital costs by a factor of 1.6 to account for additional up-front expenditures (siting, infrastructure development, pumps, electronics, etc.) following traditional water technology analyses (Malek et al., 1996; Bartholomew et al., 2018). Operational costs are comprised of electricity, brine disposal, and labor/maintenance. We model electricity

costs after rates published for small to medium businesses by the California Pacific Gas & Electric Company (PG&E, 2019), and we account for hourly and seasonal variations. Traditional CDI techno-economic analyses typically neglect brine disposal costs due to the low salinity feeds commonly associated with CDI. However, for completeness, we will include disposal costs in this analysis. For brackish water desalination with  $c_0 = 20$  mM and an average brine concentration of 29.6 mM ( $\Delta c = 9.6$  mM) we assume a brine disposal cost of  $\$0.02 \text{ m}^{-3}$ . Labor is estimated to be 3% of the total capital cost of the plant following analyses of comparable water technologies (Vince et al., 2008; Bartholomew et al., 2018; Hand et al., 2019a). Further, we consider a CDI plant which has a 5-year lifespan and operates 90% of the time each year. Table 2 lists all economic parameters and unit costs used in the following analysis.

**Table 2** Parameters and cost parameters used for electrode aging economics studies

Parameter	Value	Ref
Discount rate, $i$	6.6 %	assumed
Plant lifetime	5 y	assumed
Plant load factor	90% uptime	(Malek et al., 1996; Bartholomew et al., 2018; Hand et al., 2019a)
Electrode cost	$\$1, 6, 10 \text{ m}^{-2}$	estimated from Hand et al. (2019a)
Frame/housing cost	$\$2 \text{ m}^{-2}$	(Darling et al., 2014; Hand et al., 2019a)
Separator cost	$\$2 \text{ m}^{-2}$	(Darling et al., 2014; Hand et al., 2019a)
Current collector cost	$\$5 \text{ m}^{-2}$	(Darling et al., 2014; Hand et al., 2019a)
Electricity cost	Time varying, $\$0.22\text{-}0.29 \text{ kWh}^{-1}$	(PG&E, 2019)
Brine disposal cost	$\$0.02 \text{ m}^{-3}$	estimated
Labor/maintenance	3% CC $\text{y}^{-1}$	(Vince et al., 2008; Bartholomew et al., 2018; Hand et al., 2019a).

Fig. 4 plots fractions of costs which comprise overall water desalination costs for CDI predicted by our model. We vary the electrode unit cost to be (a)  $\$10 \text{ m}^{-2}$  (b)  $\$6 \text{ m}^{-2}$  and (c)  $\$1 \text{ m}^{-2}$  each

and consider electrode replacement frequencies of 1, 3, and 5 replacements over the plant's 5-year lifetime. Displayed above each bar is the resulting levelized cost of water for each condition. For this study we consider a constant flow rate, sinusoidal current (at system resonance,  $\omega_{res} = 1/\sqrt{\tau RC}$ ) operating condition with  $c_0 = 20$  mM,  $\Delta c = 9.6$  mM,  $WR = 0.5$ ,  $P = 6$  L m<sup>-2</sup> h<sup>-1</sup>, and  $E_v = 0.32$  kWh m<sup>-3</sup>.

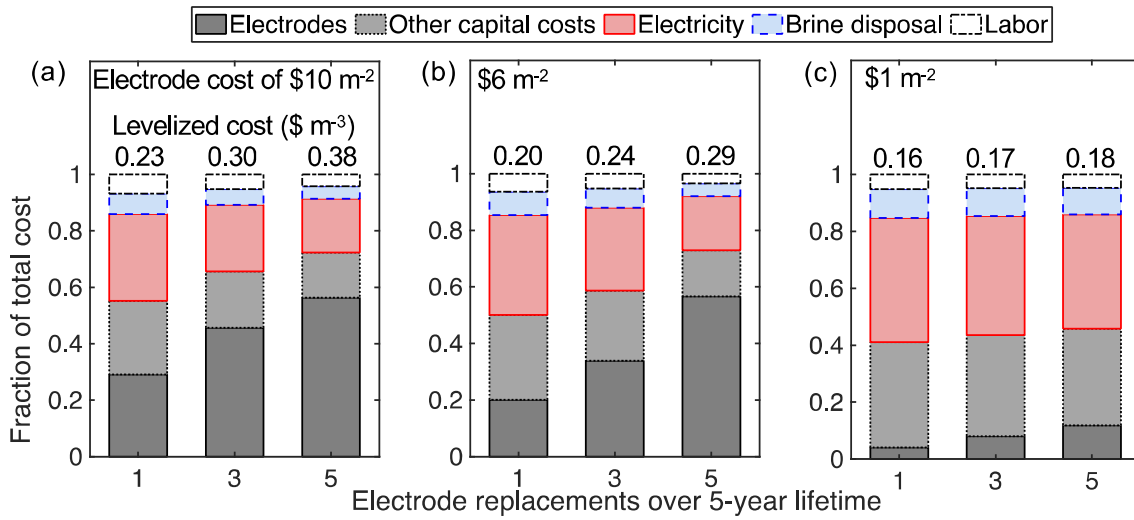


**Fig. 4.** Key contributions to CDI levelized cost of water ( $LC$ ) as a function of electrode cost and replacement frequency predicted by our model. Plotted are fractional contributions of energy, brine disposal, labor/maintenance, electrodes, and other capital costs to  $LC$  (label above each bar) over a 5-year plant lifetime. We assume carbon electrode unit costs of (a)  $\$10$  m<sup>-2</sup> (b)  $\$6$  m<sup>-2</sup> and (c)  $\$1$  m<sup>-2</sup> each and electrode replacement frequencies of 1, 3, and 5 replacements per lifetime. For electrode costs  $\$6$  m<sup>-2</sup> and higher ((a) and (b)), capital and electrode costs comprise at least half of  $LC$ . The value of  $\$6$  m<sup>-2</sup> (b) constitutes the transition point between dominance of capital and material cost (a) versus operational cost (c). For all cases, costs are given as a present worth with  $i = 6.6\%$  under the operating conditions:  $c_0 = 20$  mM,  $\Delta c = 9.6$  mM,  $WR = 0.5$ ,  $P = 6$  L m<sup>-2</sup> h<sup>-1</sup>, and  $E_v = 0.32$  kWh m<sup>-3</sup>.

As expected, the predicted data of Fig. 4 indicate that the relative importance of electrode costs increasingly dominate levelized costs as electrode replacement frequency is increased. For example, in **Fig. 4 a**, electrodes (a  $\$10 \text{ m}^{-2}$  electrode cost) and other capital costs comprise roughly 70% of the  $\$0.38 \text{ m}^{-3}$  levelized cost for one replacement per year. On the other hand, Fig. 4c (a  $\$1 \text{ m}^{-2}$  electrode cost) suggests these constitute only 40% of the  $\$0.16 \text{ m}^{-3}$  LC for a replacement every 5 y. In comparison to previous studies, we note Yu et al. (2016) assumed a 1 y electrode lifetime, while Hand et al. (2019a) reported a levelized cost of roughly  $\$0.38 \text{ m}^{-2}$  for non-membrane CDI with an electrode and overall plant lifetime of 2 y. The data presented here strongly suggest that existing CDI economics are likely dominated by capital and material costs (versus energy and other operational costs) and so improvements in electrode aging can have significant impact on CDI water levelized cost. Note also that the data of Fig. 4 is independent of the mechanism by which electrodes age (only the resulting replacement frequency). We will next explore specific aging mechanisms.

#### *4.3. Techno-economic analysis: evaluating the effect of electrode aging and replacement criteria on the overall levelized cost of water*

We here hypothesize two practically relevant mechanisms that drive electrode aging, and then formulate these mechanisms into our techno-economic model. In addition to aging criteria, this analysis explores the effects of CDI operation and electrode cost on levelized cost. We emphasize that, while this analysis focuses on resulting levelized cost, the calculations are applicable to the study of the effects CDI operational modes have on electrode replacement costs. For simplicity, we neglect fouling but note that fouling and feedwater composition can be a significant electrode aging mechanism (Liu et al., 2019 suggested fouling can be mitigated

through upstream water conditioning and electrode cleaning). The first hypothesized criterion is an electrode lifetime based on the number of electrical charge/discharge cycles. This hypothesis is simple and could be coded into the controller of a CDI cell.

For the second criterion, we posit that electrode aging is governed by the cumulative time of operation above a certain value of applied total cell potential. This hypothesis is informed by the studies of Cohen et al. (2013) and Lu et al. (2017) which showed that operation at reduced cell potentials (below 0.7 V for the former and 0.8 V for the latter) significantly delayed electrode oxidation when compared to operation at higher and more commonly used applied potentials (e.g. 1.2 V). Also, experiments performed by Cohen et al. (2015) implemented an alternating polarization operation mode between  $\pm 0.9$  V, and showed retained adsorption concentration and cell stability after 816 h of continuous operation. We thus hypothesize that electrode degradation is related to the time spent at higher potentials. For the present study, we chose operation time spent at cell potential above a threshold of 0.8 V as one aging and electrode replacement criterion. In future work, we hope to study the effects of electrode oxidation and the related issue of the effects of surface functionalities on electrode aging (Li et al., 2020). In Section S4 of the SI we present a third hypothesis for electrode aging which considers only operational time (electrodes replaced every 1 y). This type of replacement criterion has been used in CDI techno-economic and lifecycle analyses as a baseline estimate (Yu et al., 2016; Hand et al., 2019a). We stress that the simulation and technoeconomic analysis tool described here is useful in making comparisons among these and other aging criteria on the levelized cost of water.



Fig. 5a and b show plots of levelized cost versus  $P$  and  $\Delta c$  subject to the two aforementioned electrode aging hypotheses. Fig. 5a shows levelized cost for electrodes replaced every 500 h of operation above a voltage threshold of 0.8 V, while Fig. 5b shows costs for electrodes replaced every 24,000 cycles. The value of 500 h is encapsulated by the study performed by Cohen et al. (2015) and the value of 24,000 cycles was selected to result in electrode replacement frequencies from 0 to 6 per plant lifetime, encapsulating the analysis of Fig. 4. Note all related parameters can be specified by the user. As before, we consider a constant flow rate, resonant sinusoidal current operating condition with  $c_0 = 20$  mM. However, we here expand the operational regime to include desalination depths of  $\Delta c \in [3,11]$  mM and productivities  $P \in [3,18]$  L m<sup>-2</sup> h<sup>-1</sup>. Areas marked as “not feasible” represent operational regimes where a given desalination depth is not attainable for a fixed productivity with a voltage window below 1.2 V. In Fig. 5c we reduce the unit cost of electrodes to \$1 m<sup>-2</sup>, a regime where levelized cost is more strongly affected by operational costs.

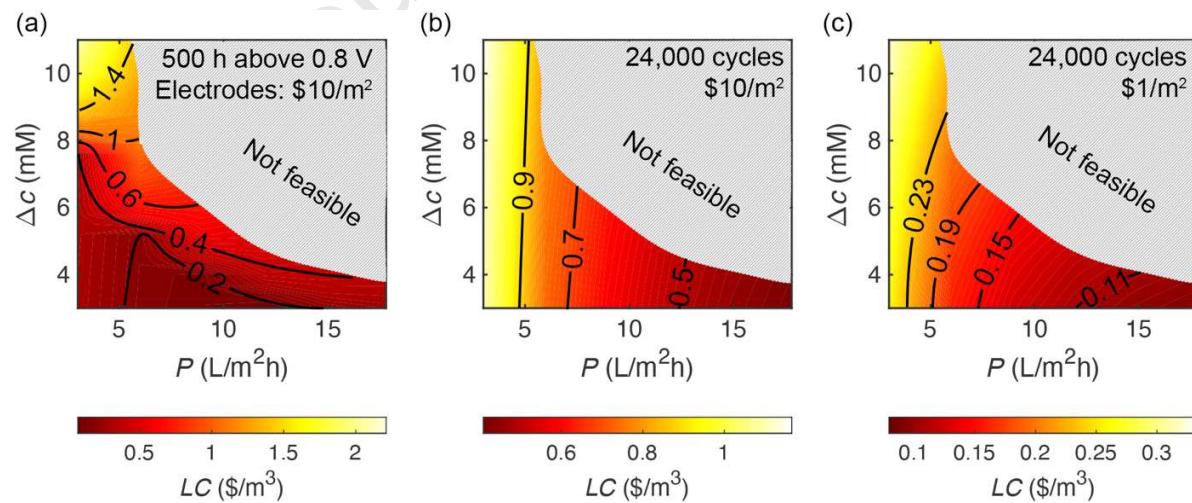


**Fig. 5.** Levelized cost (cost per volume of produced desalinated water) as a function of productivity  $P$  and volume-averaged desalination depth  $\Delta c$  for two electrode replacement

criteria: (a) assumes replacement every 500 h of operation above 0.8 V while (b) shows replacement after 24,000 cycles. Plot (c) shows the same replacement criterion as (b) but for a theorized electrode cost of just  $\$1 \text{ m}^{-2}$ . Operating conditions are constant flow rate with resonant sinusoidal forcing current, and peak voltage varies to meet demand for  $P$  and  $\Delta c$ .  $c_0 = 20 \text{ mM}$ , and plant lifetime is 5 y with a 90% uptime. Levelized cost depends on both  $P$  and  $\Delta c$  in (a) as salt separation and water throughput requirements both modulate required time spent above 0.8 V. In contrast,  $LC$  in (b) is roughly inversely proportional to  $P$  (and insensitive to  $\Delta c$ ) since operational costs are negligible. For (c), electrode costs are small enough that again the manner of operation (particularly higher voltage values influencing energy consumption) is important and so  $LC$  again depends on  $P$  and  $\Delta c$ .

For the electrode aging criterion based on time spent above 0.8 V, Fig. 5a shows that  $LC$  is determined by both desalination depth and water throughput. We see that  $LC$  decreases monotonically with decreasing  $\Delta c$ . Demand for  $\Delta c$  above about 8 mM increases  $LC$  and strongly limits the feasible  $P$  range. Interestingly, a demand for increased productivity can either decrease or increase  $LC$ ; this reflects the competing influence between electrode replacement and total water production. For example, for  $\Delta c$  at values between about 3 and 5 mM,  $LC$  exhibits a local minimum for increasing  $P$  (e.g. a minimum value of  $\$0.13 \text{ m}^{-3}$  for  $\Delta c = 4 \text{ mM}$  and  $P = 8 \text{ L m}^{-2} \text{ h}^{-1}$ ). Initially, increases in  $P$  drive (for constant  $\Delta c$ ) lower levelized cost. Past the local minimum,  $LC$  increases as increases in productivity drive more frequent electrode replacements (since operation requires higher peak voltages to maintain the constant  $\Delta c$ ).

Fig. 5b shows  $LC$  for the second criterion associated with 24,000 cell cycles and a  $\$10 \text{ m}^{-2}$  electrode cost. Within the feasible region, the cycle-based electrode replacement criterion is exactly independent of the voltage values imposed in the cell and energy costs are approximately negligible. That is, a higher operational voltage window required for increased desalination depth at a given productivity does not decrease electrode life. Hence, the electrode replacement cost is high enough that  $LC$  is driven by a ratio of the present worth of capital costs (including electrodes) and the amount of water produced (and so  $LC$  is approximately inversely proportional to  $P$ ). In Fig. 5c, the electrode cost is sufficiently low ( $\$1 \text{ m}^{-2}$ ) such that energy costs are again important to  $LC$ . Here,  $LC$  depends more strongly on both  $P$  and  $\Delta c$ , and the lowest  $LC$  of all cases is achievable for low  $\Delta c$  (lowering energy costs) and high productivity (increasing amount of produced water).

$LC$  is an important metric in comparing among economic feasibility of various desalination technologies. For example,  $LC$  for electrodialysis (ED) has been reported at about  $\$0.60 \text{ m}^{-3}$  for brackish feed water desalination (Younos, 2009; Mezher et al., 2011). Reported values for RO systems applied to brackish water desalination range from about  $\$0.20$  to  $0.70 \text{ m}^{-3}$  (Younos, 2009; Mezher et al., 2011). Of course, such comparisons are not easily made as these  $LC$ s depend on operating conditions such as initial concentration, decreases in concentration, and throughput, as well as operating modes. For example, energy consumption (an important contributor to  $LC$ ) by ED is reported to be a function of amount and rate of salt removed (Turek, 2003). Also, RO energy consumption also depends on initial salinity as well as flow rate (therefore throughput) and membrane type which, in turn, influences pumping pressure (Lee et al., 2011; Li, 2011). Further, RO is typically applied to higher salinity feeds and achieves higher

desalination depths. Of course, membrane and/or electrode replacement costs also significantly affect the *LCs* of these technologies. Accurate and more comprehensive determination of *LC* as a function of operation for CDI motivates further work in developing and applying techno-economic tools.

## 5. Summary and conclusions

We presented a newly developed open-source CDI analysis and design program. The tool is built as an installable Matlab GUI program. Matlab's Simulink environment is used to design and build CDI systems, and the GUI is used to run the Simulink model and view results. Included are tools for physics-based modeling of one or more CDI cells and coupled techno-economic models to compute economic parameters such as levelized cost of water. The program allows for coupling of one or more CDI cells to related systems such as power conversion and disposal costs, and the techno-economic analysis converts among various dimensional streams of species (e.g. feed, desalted water, and brine), energy, and cost. The physics-based model was validated by quantitative comparison to experimental CDI data from laboratory experiments. We demonstrated the program in performing two distinct CDI design and analysis investigations.

The physics-based program was used to simulate CDI dynamics subject to sinusoidal flow rate operation. The investigation analyzed the effects of varying flow rate amplitude and phase offset with respect to a sinusoidal current electrical input, including independent variation of flow rate sinusoid amplitude and phase on water recovery ratio, productivity, volumetric energy consumption, and volume-averaged desalination depth. We observed desalination depth is achieved at the expense of the other three figures of merit (similar to the case of constant flow

rate). The model enables analyses of arbitrary flow rate and electric forcing in CDI and may aid in development of new and optimized CDI operation strategies.

As relevant techno-economic analyses, we explored electrode lifetime and replacement criteria on levelized cost of produced water. The analyses suggest that electrode costs in CDI are currently a greater contributor than operational costs (e.g. electrical energy input) to overall levelized cost of produced water. The model was also used to study the effects of three plausible electrode aging mechanisms on the levelized cost of water: operation time above 0.8 V (to account for electrode oxidation) versus simple number of cycles operation. In the SI, we presented operational time as a third aging criterion. Our study highlights the importance of further research toward identifying electrode aging mechanisms and development of operational methods which extend electrode lifetimes. Of course, decreasing of electrode costs remains an important challenge in CDI.

## Acknowledgements

T.D.H., W.A.T., and J.G.S. gratefully acknowledge funding from Stanford Tomkat Center for Sustainable Energy. A.R. gratefully acknowledges funding from the Bio-X Bowes Fellowship of Stanford University. Work at LLNL was performed under the auspices of the US DOE by LLNL under Contract DE-AC52-07NA27344.

## References

- Bartholomew, T. V., Siefert, N.S., Mauter, M.S., 2018. Cost Optimization of Osmotically Assisted Reverse Osmosis. *Environ. Sci. Technol.* <https://doi.org/10.1021/acs.est.8b02771>
- Biesheuvel, P.M., Van Limpt, B., Van Der Wal, A., 2009. Dynamic adsorption/desorption process model for capacitive deionization. *J. Phys. Chem. C.* <https://doi.org/10.1021/jp809644s>
- Biesheuvel, P.M., Zhao, R., Porada, S., van der Wal, A., 2011. Theory of membrane capacitive deionization including the effect of the electrode pore space. *J. Colloid Interface Sci.* <https://doi.org/10.1016/j.jcis.2011.04.049>
- Cohen, I., Avraham, E., Bouhadana, Y., Soffer, A., Aurbach, D., 2015. The effect of the flow-regime, reversal of polarization, and oxygen on the long term stability in capacitive de-ionization processes. *Electrochim. Acta.* <https://doi.org/10.1016/j.electacta.2014.12.007>
- Cohen, I., Avraham, E., Bouhadana, Y., Soffer, A., Aurbach, D., 2013. Long term stability of capacitive de-ionization processes for water desalination: The challenge of positive electrodes corrosion. *Electrochim. Acta.* <https://doi.org/10.1016/j.electacta.2013.05.029>
- Darling, R.M., Gallagher, K.G., Kowalski, J.A., Ha, S., Brushett, F.R., 2014. Pathways to low-cost electrochemical energy storage: A comparison of aqueous and nonaqueous flow batteries. *Energy Environ. Sci.* <https://doi.org/10.1039/c4ee02158d>
- Demirer, O.N., Naylor, R.M., Rios Perez, C.A., Wilkes, E., Hidrovo, C., 2013. Energetic performance optimization of a capacitive deionization system operating with transient cycles and brackish water. *Desalination.* <https://doi.org/10.1016/j.desal.2013.01.014>
- Dykstra, J.E., Porada, S., van der Wal, A., Biesheuvel, P.M., 2018. Energy consumption in capacitive deionization – Constant current versus constant voltage operation. *Water Res.*

<https://doi.org/10.1016/j.watres.2018.06.034>

Hand, S., Guest, J.S., Cusick, R.D., 2019a. Technoeconomic Analysis of Brackish Water

Capacitive Deionization: Navigating Tradeoffs between Performance, Lifetime, and

Material Costs. *Environ. Sci. Technol.* <https://doi.org/10.1021/acs.est.9b04347>

Hand, S., Shang, X., Guest, J.S., Smith, K.C., Cusick, R.D., 2019b. Global Sensitivity Analysis

to Characterize Operational Limits and Prioritize Performance Goals of Capacitive

Deionization Technologies. *Environ. Sci. Technol.* <https://doi.org/10.1021/acs.est.8b06709>

Hawks, S.A., Knipe, J.M., Campbell, P.G., Loeb, C.K., Hubert, M.A., Santiago, J.G.,

Stadermann, M., 2018. Quantifying the flow efficiency in constant-current capacitive

deionization. *Water Res.* <https://doi.org/10.1016/j.watres.2017.11.025>

Hawks, S.A., Ramachandran, A., Porada, S., Campbell, P.G., Suss, M.E., Biesheuvel, P.M.,

Santiago, J.G., Stadermann, M., 2019. Performance metrics for the objective assessment of

capacitive deionization systems. *Water Res.* <https://doi.org/10.1016/j.watres.2018.10.074>

Hemmatifar, A., Palko, J.W., Stadermann, M., Santiago, J.G., 2016. Energy breakdown in

capacitive deionization. *Water Res.* <https://doi.org/10.1016/j.watres.2016.08.020>

Kim, T., Yoon, J., 2015. CDI ragone plot as a functional tool to evaluate desalination

performance in capacitive deionization. *RSC Adv.* <https://doi.org/10.1039/c4ra11257a>

Lee, K.P., Arnot, T.C., Mattia, D., 2011. A review of reverse osmosis membrane materials for

desalination-Development to date and future potential. *J. Memb. Sci.*

<https://doi.org/10.1016/j.memsci.2010.12.036>

Li, B., Zheng, T., Ran, S., Sun, M., Shang, J., Hu, H., Lee, P.H., Boles, S.T., 2020. Performance

Recovery in Degraded Carbon-Based Electrodes for Capacitive Deionization. *Environ. Sci.*

*Technol.* <https://doi.org/10.1021/acs.est.9b04749>

- 578 Li, M., 2011. Reducing specific energy consumption in Reverse Osmosis (RO) water  
 579 desalination: An analysis from first principles. *Desalination*.  
 580 <https://doi.org/10.1016/j.desal.2011.03.031>
- 581 Liu, X., Shanbhag, S., Mauter, M.S., 2019. Understanding and mitigating performance decline in  
 582 electrochemical deionization. *Curr. Opin. Chem. Eng.*  
 583 <https://doi.org/10.1016/j.coche.2019.07.003>
- 584 Lu, D., Cai, W., Wang, Y., 2017. Optimization of the voltage window for long-term capacitive  
 585 deionization stability. *Desalination*. <https://doi.org/10.1016/j.desal.2017.09.026>
- 586 Malek, A., Hawlader, M.N.A., Ho, J.C., 1996. Design and economics of RO seawater  
 587 desalination. *Desalination*. [https://doi.org/10.1016/0011-9164\(96\)00081-1](https://doi.org/10.1016/0011-9164(96)00081-1)
- 588 Mezher, T., Fath, H., Abbas, Z., Khaled, A., 2011. Techno-economic assessment and  
 589 environmental impacts of desalination technologies. *Desalination*.  
 590 <https://doi.org/10.1016/j.desal.2010.08.035>
- 591 Newman, D.G., Lavelle, J.P., Eschenbach, T.G., 2015. *Engineering Economic Analysis:*  
 592 *Engineering Costs [WWW Document]. Oxford Univ. Press.*
- 593 Oren, Y., 2008. Capacitive deionization (CDI) for desalination and water treatment - past,  
 594 present and future (a review). *Desalination*. <https://doi.org/10.1016/j.desal.2007.08.005>
- 595 Oyarzun, D.I., Hawks, S.A., Campbell, P.G., Hemmatifar, A., Krishna, A., Santiago, J.G.,  
 596 Stadermann, M., 2020. Energy transfer for storage or recovery in capacitive deionization  
 597 using a DC-DC converter. *J. Power Sources*.  
 598 <https://doi.org/10.1016/j.jpowsour.2019.227409>
- 599 Oyarzun, D.I., Hemmatifar, A., Palko, J.W., Stadermann, M., Santiago, J.G., 2018. Adsorption  
 600 and capacitive regeneration of nitrate using inverted capacitive deionization with surfactant



functionalized carbon electrodes. Sep. Purif. Technol.

<https://doi.org/10.1016/j.seppur.2017.11.027>

PG&E, 2019. Small & Medium Business Time-of-use Rate Plans [WWW Document]. Pacific

Gas Electr. Co. URL [www.pge.com](http://www.pge.com) (accessed 1.10.19).

Qin, M., Deshmukh, A., Epsztein, R., Patel, S.K., Owoseni, O.M., Walker, W.S., Elimelech, M.,

2019. Comparison of energy consumption in desalination by capacitive deionization and

reverse osmosis. Desalination. <https://doi.org/10.1016/j.desal.2019.01.003>

Qu, Y., Campbell, P.G., Gu, L., Knipe, J.M., Dzenitis, E., Santiago, J.G., Stadermann, M., 2016.

Energy consumption analysis of constant voltage and constant current operations in

capacitive deionization. Desalination. <https://doi.org/10.1016/j.desal.2016.09.014>

Ramachandran, A., Hawks, S.A., Stadermann, M., Santiago, J.G., 2018a. Frequency analysis and

resonant operation for efficient capacitive deionization. Water Res.

<https://doi.org/10.1016/j.watres.2018.07.066>

Ramachandran, A., Hemmatifar, A., Hawks, S.A., Stadermann, M., Santiago, J.G., 2018b. Self

similarities in desalination dynamics and performance using capacitive deionization. Water

Res. <https://doi.org/10.1016/j.watres.2018.04.042>

Ramachandran, A., Oyarzun, D.I., Hawks, S.A., Campbell, P.G., Stadermann, M., Santiago, J.G.,

2019. Comments on “Comparison of energy consumption in desalination by capacitive

deionization and reverse osmosis.” Desalination.

<https://doi.org/10.1016/j.desal.2019.03.010>

Suss, M.E., Porada, S., Sun, X., Biesheuvel, P.M., Yoon, J., Presser, V., 2015. Water

desalination via capacitive deionization: What is it and what can we expect from it? Energy

Environ. Sci. <https://doi.org/10.1039/c5ee00519a>

- 624 Turek, M., 2003. Cost effective electrodialytic seawater desalination. *Desalination*.  
625 [https://doi.org/10.1016/S0011-9164\(02\)01130-X](https://doi.org/10.1016/S0011-9164(02)01130-X)
- 626 Vince, F., Marechal, F., Aoustin, E., Bréant, P., 2008. Multi-objective optimization of RO  
627 desalination plants. *Desalination*. <https://doi.org/10.1016/j.desal.2007.02.064>
- 628 Wang, L., Lin, S., 2019. Theoretical framework for designing a desalination plant based on  
629 membrane capacitive deionization. *Water Res.* <https://doi.org/10.1016/j.watres.2019.03.076>
- 630 Younos, T., 2009. The Economics of Desalination. *J. Contemp. Water Res. Educ.*  
631 <https://doi.org/10.1111/j.1936-704x.2005.mp132001006.x>
- 632 Yu, T.H., Shiu, H.Y., Lee, M., Chiueh, P. Te, Hou, C.H., 2016. Life cycle assessment of  
633 environmental impacts and energy demand for capacitive deionization technology.  
634 *Desalination*. <https://doi.org/10.1016/j.desal.2016.08.007>
- 635
- 636
- 637

### **Highlights**

- A novel program to simulate capacitive deionization physics has been developed
- General flowrate and electrical input models encourage dynamic optimization
- Electrode costs are larger than operational costs for capacitive deionization
- Electrode aging studies are crucial to achieve cost optimization

**Declaration of interests**

☒ The authors declare that they have no known competing financial interests or personal relationships that could have appeared to influence the work reported in this paper.

☐ The authors declare the following financial interests/personal relationships which may be considered as potential competing interests: